Liu Yingli, Wang Jingsong*, Guo Wentao, Dong Zeshang and Xue Qingguo

Kinetics Calculation of the Non-isothermal Reduction of Pellet

DOI 10.1515/htmp-2015-0034
Received February 5, 2015; accepted May 25, 2015

Abstract: The reduction tests of pellet were carried out from room temperature to 1,373 K in the condition of traditional blast furnace (TBF) and oxygen blast furnace (OBF) by thermogravimeter measurement. The apparent activation energy E, pre-exponential factor A and the controlling steps of reaction were determined by the non-isothermal method of Coats–Redfern. In the condition of TBF, the reduction is controlled by solid diffusion to interfacial chemical reaction at initial stage, and gas diffusion at final stage. In the condition of OBF, the controlling step switched from solid diffusion to gas diffusion + interfacial chemical reaction in the beginning and the interfacial chemical reaction at the late stage. Meanwhile, the transition temperature points of the controlling step were predicted. The transition temperatures are 750 °C and 900 °C in TBF and 630 °C (earlier 120 °C than in TBF) and 900 °C (after the insulation) in OBF.

Keywords: oxygen blast furnace, non-isothermal, kinetics, pellet

Introduction

In a large part, the productivity and the fuel consumption in blast furnace are mostly dependent on the reduction degree of ferrous burden in lump zone. Improving the reducing property of ferrous burden in the upper furnace can reduce the direct reduction degree, which can achieve energy-saving and cost-reducing. In traditional blast furnace (TBF), the direct reduction degree is almost close to the theoretical minimum value [1]. Meanwhile, the oxygen blast furnace (OBF) [2], a new iron-making technology, has been confirmed by the feasibility of the industrial experiment in Japan [3], Russia [4] and Sweden [5]. The direct reduction degree can be reduced to 0.10 [6], which greatly decreases the fuel ratio. Therefore, it is necessary to study the kinetics of ferrous burden in lump zone in the condition of OBF.

The isothermal method [7, 8] has some shortcomings, such as zero time effect, cannot respond to the reduction process of burden and so on. With the continuous improvement of apparatus and the constant innovation of analysis method, the non-isothermal method [9] improved the above shortcomings. As a continuous approach, it can study the kinetic parameter in the whole reaction temperature and better reflect the reduction history. At present, many authors [10–12] have investigated the reduction kinetics in isothermal method, but few focus on that in non-isothermal method, especially in the atmosphere of OBF. In this study, the programming reduction of pellet was carried out by thermogravimeter measurement from room temperature to 1,373 K in the atmosphere of TBF and OBF. The reduction kinetic parameter, the controlling step and the transition temperature were determined by the non-isothermal Coats–Redfern equation.

***Corresponding author: Wang Jingsong,** State Key Laboratory of Advanced Metallurgy, University of Science and Technology Beijing, Beijing 100083, China, E-mail: wangjingsong@ustb.edu.cn
Liu Yingli, Guo Wentao, Dong Zeshang, Xue Qingguo, State Key Laboratory of Advanced Metallurgy, University of Science and Technology Beijing, Beijing 100083, China

Experimental

Raw material

The samples used in this experiment are pellet purchased from Laiwu Steel Company, Ltd. The chemical composition and the analysis result of XRD (X-ray diffraction) are shown in Table 1 and Figure 1. Pellet is composed of hematite and the complex compounds.

Experimental apparatus and conditions

The programming reduction experiments were carried out in a gas–solid reaction equipment with continuous measuring of weight change, as shown in Figure 2. The maximum temperature of the reaction furnace is 1,373 K. The precision of temperature controller is 1 K min^{-1}. The electronic balance connected with computer collects the weight change per 1 min. The granular size of ferrous burden is 10–12.5 mm, and the mass of sample is 500 g.

Table 1: Chemical compositions of pellet (mass.%).

TFe	FeO	CaO	MgO	Al_2O_3	SiO_2	TiO_2	S	R
62.46	3.69	1.06	0.97	1.50	7.62	0.17	0.005	0.14

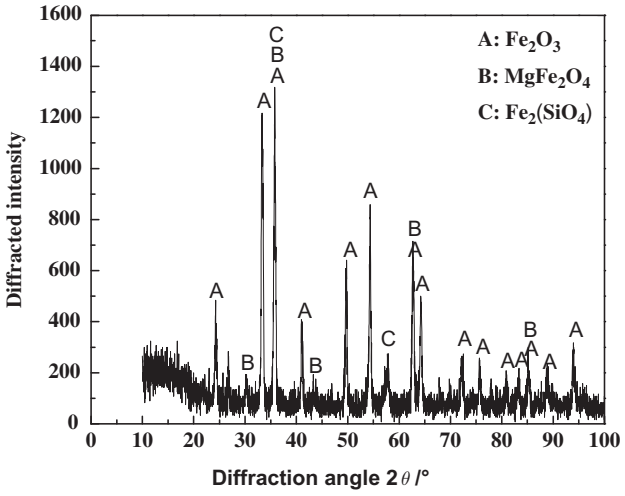

Figure 1: X-ray diffraction patterns

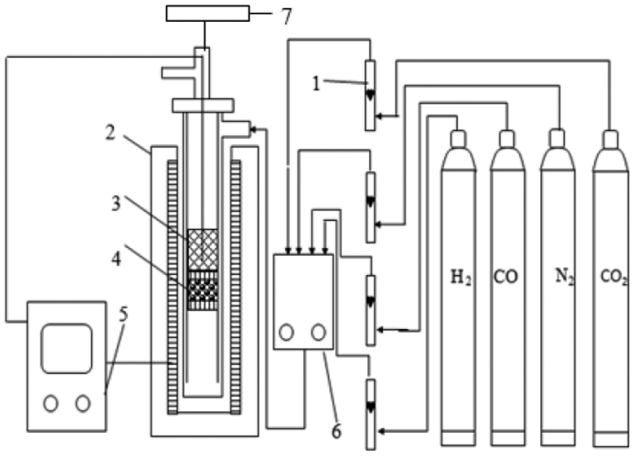

Figure 2: Experimental apparatus: 1, gas flow meter; 2, heating furnace; 3, burden; 4, high alumina ball; 5, temperature controlled box; 6, gas flow controller; 7, electric balance.

The sample was dried for 3 h in 120 °C, and then was tiled in the bottom of furnace.

Figure 3 shows the temperature system and the gas composition variation in different zone. First, the flow rate is 5 L/min high purity N_2 before 200 °C. Second, the gas flow was switched to 15 L/min mixed reduction gas. The gas composition variation occurs at 750 °C, 900 °C and after the 900 °C insulation. Third, when the temperature arrived at 1,100 °C, the power was cut off. The mixed reduction gas was switched to 5 L/min high-purity N_2 to protect the samples from reoxidation.

Data calculation

According to the composition of pellet, the total theoretical mass loss is constant when pellet was reduced completely. The conversion rate α [13–15] is the ratio of mass loss after t min and the total theoretical mass loss. The calculation is as follows:

$$\alpha = \frac{m_0 - m_t}{m_e} \tag{1}$$

In eq. (1), α stands for the conversion rate; m_0 is the initial sample weight, g; m_t is the sample mass after t min, g; m_e represents the theoretical oxygen loss, g.

By the Coats–Redfern method, the apparent activation energy and the pre-exponential factor were determined. The formula is as follows [9]:

$$\ln\left(\frac{-\ln f(\alpha)}{T^2}\right) = \ln\left[\frac{AR}{\beta E}\left(1 - \frac{2R}{E}\right)\right] - \frac{E}{RT} \tag{2}$$

In eq. (2), $f(\alpha)$ is a function that represents the reaction model; R is gas constant, 8.314 J mol^{-1} K^{-1}; β is the heating rate, K min^{-1}; E represents the apparent activation energy, J mol^{-1}; A represents the pre-exponential factor, s^{-1}; T is the temperature, K.

In general, the apparent activation energy is about thousands of Joule or dozens of kilojoules. The item in eq. (2) is $1 - \frac{2R}{E} \approx 1$. As a consequence, under the condition of a constant heating rate β and the special mechanism function $f(\alpha)$, $\ln\left(\frac{-\ln f(\alpha)}{T^2}\right)$ and $\frac{1}{T}$ were fitted a straight line. The slope and intercept of the line are $-\frac{E}{R}$ and $\ln\frac{AR}{\beta E}$, respectively. Then the apparent activation energy and pre-exponential factor can be determined.

Results and discussion

Results of tests

Figure 4 presents the variation of conversion rate with reaction time in OBF and TBF. The results show that the starting reduction temperature of pellet is 637 °C and 487 °C in TBF and OBF, respectively. It is obvious that the initial reduction potential $\left(\frac{CO+H_2}{CO+CO_2+H_2+H_2O}\right)$ in OBF is

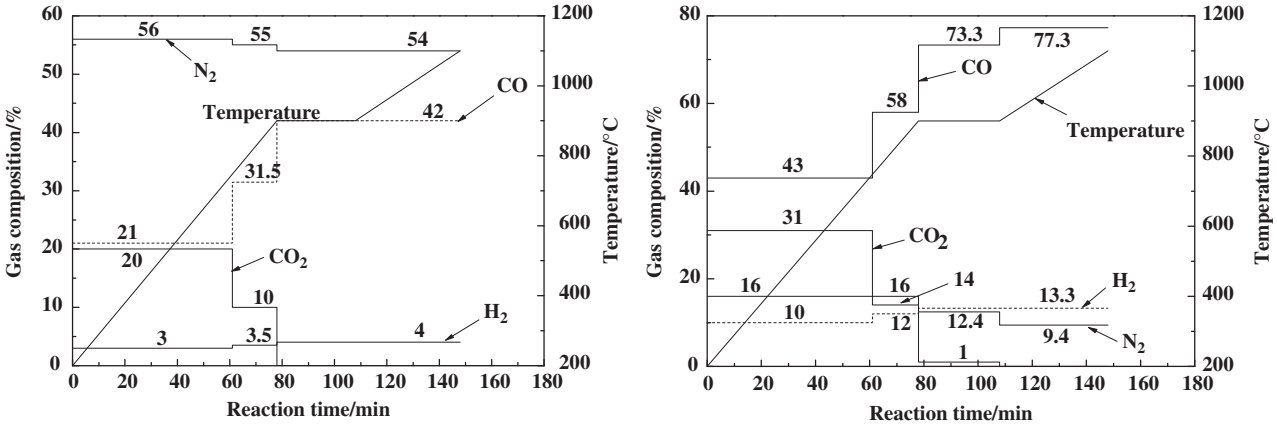

Figure 3: Temperature system and gas composition at different stages: (a) in the condition of traditional blast furnace and (b) in the condition of oxygen blast furnace.

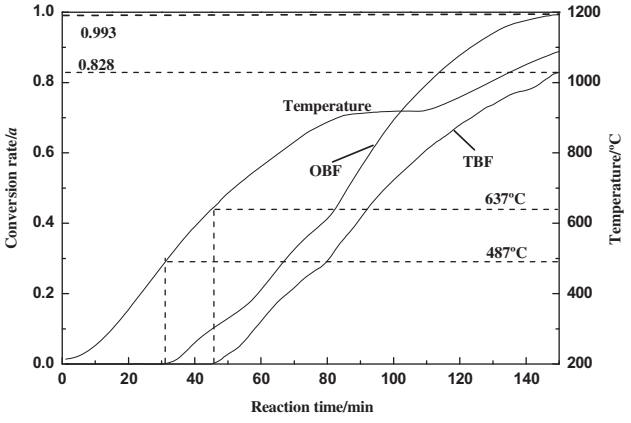

Figure 4: Variation of conversion rate with reaction time in TBF and OBF.

higher than that in TBF. Meanwhile, the final conversion rate is 0.993 and 0.828 in TBF and OBF. When the pellet was reduced to Fe_3O_4, the theoretical conversion rate (from eq. (1)) is 0.215. When the pellet was reduced to FeO, the theoretical conversion rate is 0.323.

From thermodynamic analysis, iron oxide reduction is carried out according to a certain order. The key and hardest reaction is the reduction of FeO. With reference to previous work [16–18], the reduction of pellet can be considered as the apparent first-order reaction. So the reaction function $f(\alpha)$ is equal to $1-\alpha$. According to the basic eq. (2), the formula of Coats–Redfern is as follows:

$$\ln\left(\frac{-\ln(1-\alpha)}{T^2}\right) = \ln\frac{AR}{\beta E} - \frac{E}{RT} \tag{3}$$

Defining $F(\alpha)=\ln\left(\frac{-\ln(1-\alpha)}{T^2}\right)$, put the conversion rate and the corresponding temperature into eq. (3). Then make the line of $F(\alpha)$–$\frac{1}{T}$. The slope and intercept are a and b. Linear related coefficient is R. Finally it can ask for E and A: $E = -R \times b$ and $A = \frac{\beta E e^{\alpha}}{R}$.

Kinetic calculation in the condition of TBF

From Figure 4, the reaction starting temperature of pellet is 637 °C in the condition of TBF. So the temperature range in the calculation is 637–1,100 °C. The result of non-isothermal kinetic calculation is shown in Figure 5 at 637–1,100 °C.

In Figure 5, it is obvious to find that the curve is not straight, but three stages. The first stage (1) is the range of 637–900 °C at the rate of 9 °C·min^{-1}; the second stage (2) is the 900 °C insulation zone. In this zone, it should be a vertical line. But there is the fluctuation of temperature to some extent. So it is a very steep slash. The third stage (3) is the range of 900–1,100 °C at the rate of 5 °C min^{-1}. The kinetic parameter at three stages will be calculated as follows.

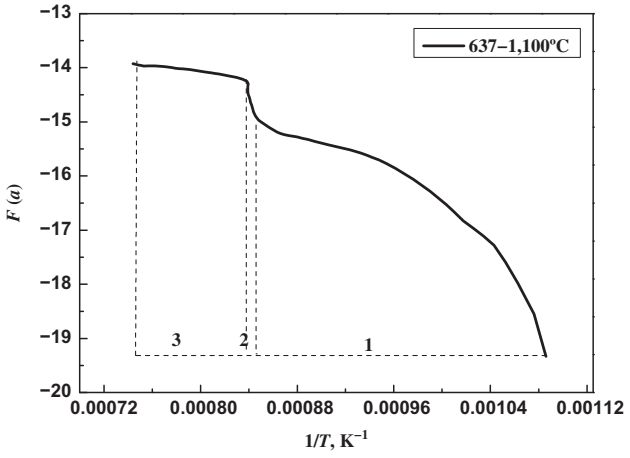

Figure 5: Calculation curve at 637–1,100 °C in TBF.

The reduction in (1) and (3) stages were carried out at constant heating rate. Using the method of Coats–Redfern, the results of calculation curve and fitting straight line were shown in Figure 6 in TBF. From Figure 6 (1), the fitting situation is bad and it is obvious to be divided into two straight lines. This is estimated to be due to the fact that the reduction potential at 750 °C was greatly improved from Figure 3. So the first stage can be divided into two stages: 637–750 °C (a) and 750–900 °C (b). Then calculate and fit the two stages, respectively. The results are shown in Figure 7.

The relevant parameters in calculation curves and fitting straight lines at different stages are shown in Table 2. From Table 2, the initial reaction activation energy is high and reaches to 168.243 kJ mol^{-1}. This phenomenon is due to the fact that the temperature and reduction potential are in the lower range at the initial

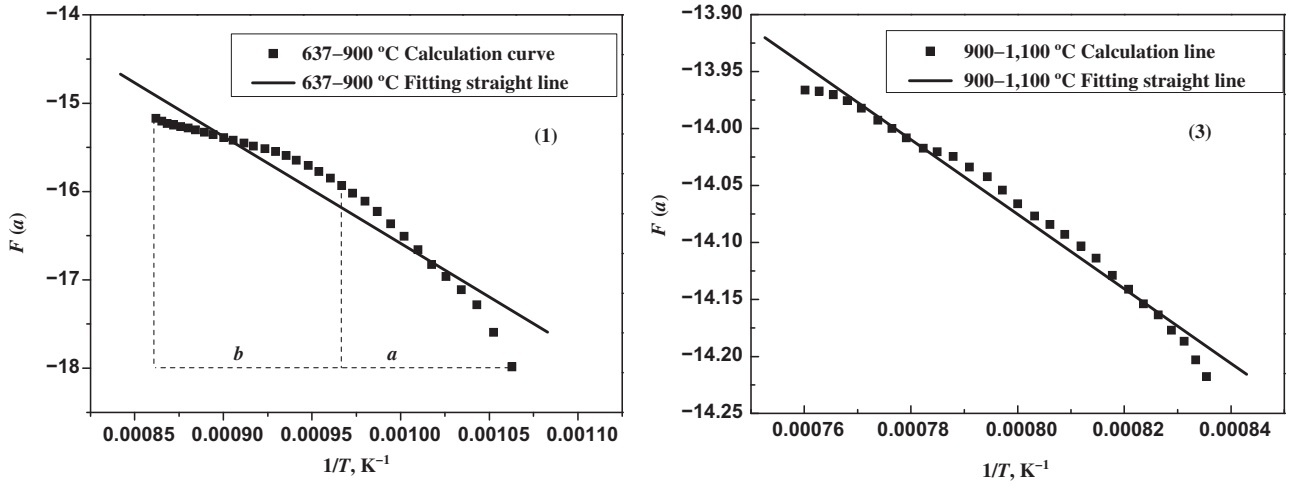

Figure 6: Calculation curve and fitting straight line at (1) and (3) stages in traditional blast furnace.

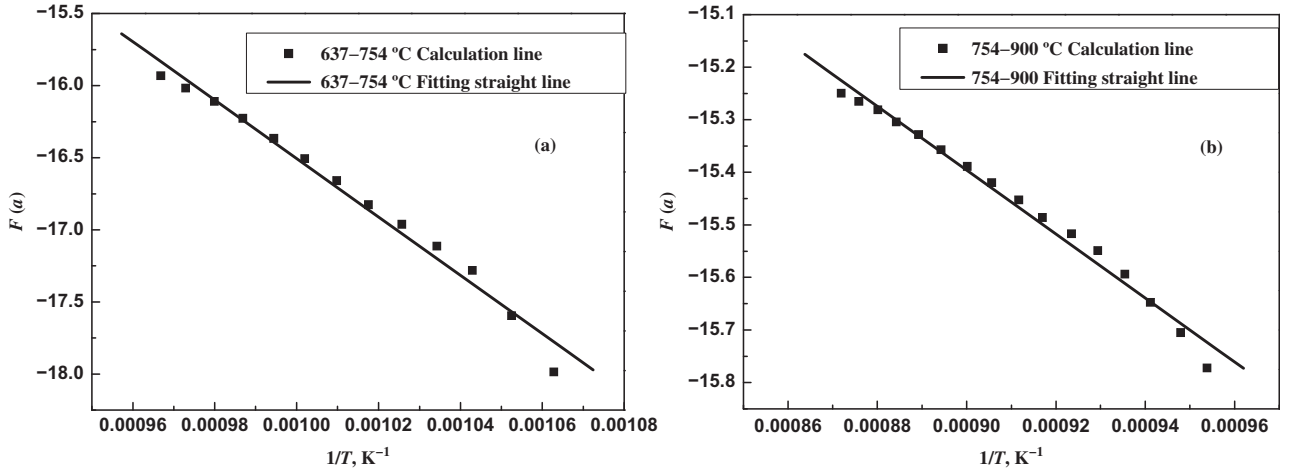

Figure 7: Calculation curves and fitting straight lines in (a) and (b) stages at 637–900 °C in TBF.

Table 2: Relevant parameters at different stages in traditional blast furnace.

Temperature range	Heating rate (°C min^{-1})	*a*	*b*	*E* (kJ mol^{-1})	*A*	*R*
637–750 °C	9	3.7304	−20,236.17 ± 810.81	168.243 ± 6.741	75,93,868	0.9913
750–900 °C	9	−9.9234	−6,080.66 ± 195.77	50.554 ± 1.628	2.68	0.9928
900–1,100 °C	5	−11.4584	−3,270.99 ± 90.89	27.195 ± 0.756	0.31	−0.9901

stage. In this stage it is the induction period and needs to overcome the largest energy barrier. But it is only 13 min. With the rise of temperature, the reduction potential was greatly improved. The apparent activation energy decreased to 50.554 kJ mol^{-1}. Under the condition of high temperature 900–1,100 °C and higher reduction potential, the activation energy is only 27.195 kJ mol^{-1}.

Corresponding relationships [19] between the values of apparent activation energy and the rate controlling steps of the reaction are shown in Table 3 [11]. According to the results of Table 3, the data in Table 2 were analyzed as follows. At the initial reaction stage, the apparent activation energy E is 168.243 kJ mol^{-1} > 90 kJ mol^{-1}. The controlling step is solid diffusion. This is due to the fact that the reaction was carried out in the outermost shell. The gas diffusion and interfacial reaction will not be the controlling step, but the diffusion of oxygen ions in solid iron oxide controls the reaction. Because of the increasing of temperature and reduction potential at 750–900 °C, the apparent activation energy is only 50.554 kJ mol^{-1}. At this range the reaction controlling step is interfacial reaction. As the reaction proceeds, the thicker the layer of production is, the greater the resistance of gas diffusion is. But the higher the temperature is, the smaller the resistance of interfacial reaction. Finally the resistance of gas diffusion exceeds that of interfacial reaction. The apparent activation energy reduced to 27.195 kJ mol^{-1} at 900–1,100 °C.

Table 3: Corresponding relationship between the values of apparent activation energy and the rate controlling steps of the reaction.

Possible controlling step	Gas diffusion	Gas diffusion + Interfacial reaction	Interfacial reaction	Solid diffusion
Apparent activation energy, E/(kJ mol^{-1})	8.0–28.0	28.0–50.0	50.0–75.0	>90

At the 900 °C insulation zone for 30 min, the controlling step was determined according to the unreacted core model. Make the line $1-(1-\alpha)^{\frac{1}{3}}$ versus t and $1-3(1-\alpha)^{\frac{2}{3}}+2(1-\alpha)$ versus t. The results are shown in Figure 8. Based on the fitting situation, the controlling step in insulation stage is gas diffusion and interfacial reaction.

Within the entire temperature range, the transition temperature points of the controlling step are 750 °C and 900 °C. Below 754 °C, the controlling step is solid diffusion. Between 754 °C and 900 °C, it is interfacial reaction.

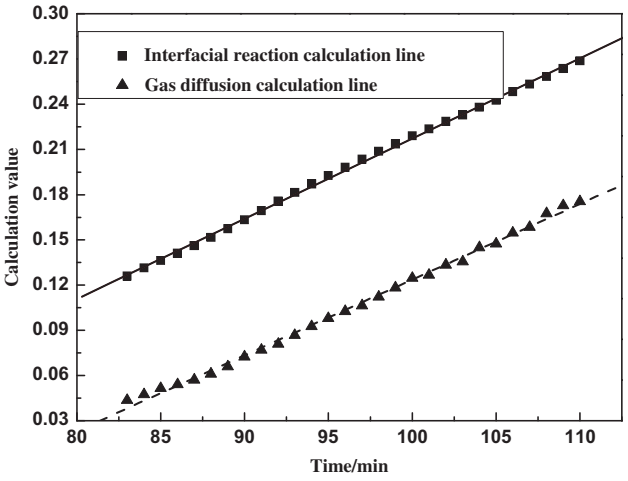

Figure 8: Fitting results of gas diffusion and interfacial reaction at the insulation stage in traditional blast furnace.

In the insulation zone, it is the mixed control of interfacial reaction and gas diffusion; since then it is gas diffusion.

Kinetic calculation in the condition of OBF

From Figure 4, the reaction starting temperature of pellet is 487 °C in the condition of OBF. So the temperature range is 487–1,100 °C in the calculation. The result of non-isothermal kinetic calculation at 487–1,100 °C is shown in Figure 9.

From Figure 9, it is similar to that in TBF. The three stages are (1) 487–900 °C at the rate of 9 °C·min^{-1}, (2) the 900 °C insulation zone and (3) 900–1,100 °C at the rate of 5 °C min^{-1}, respectively.

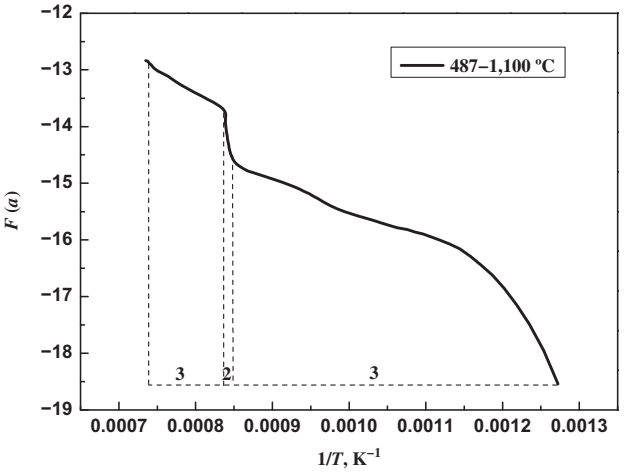

Figure 9: Calculation curve at 487–1,100 °C in OBF.

The results of calculation curve and fitting straight line at (1) and (3) stages in OBF were shown in Figure 10. There is one temperature point at 750 °C in stage (1) as in TBF. However, below 750 °C the reduction potential is higher than that in TBF. The reduction starting temperature is lower, which led to the different slope curves. So the first stage can be divided into three stages: 487–630 °C (a), 630–754 °C (b) and 754–900 °C (c). Then calculate and fit the two stages, respectively. The results are shown in Figure 11.

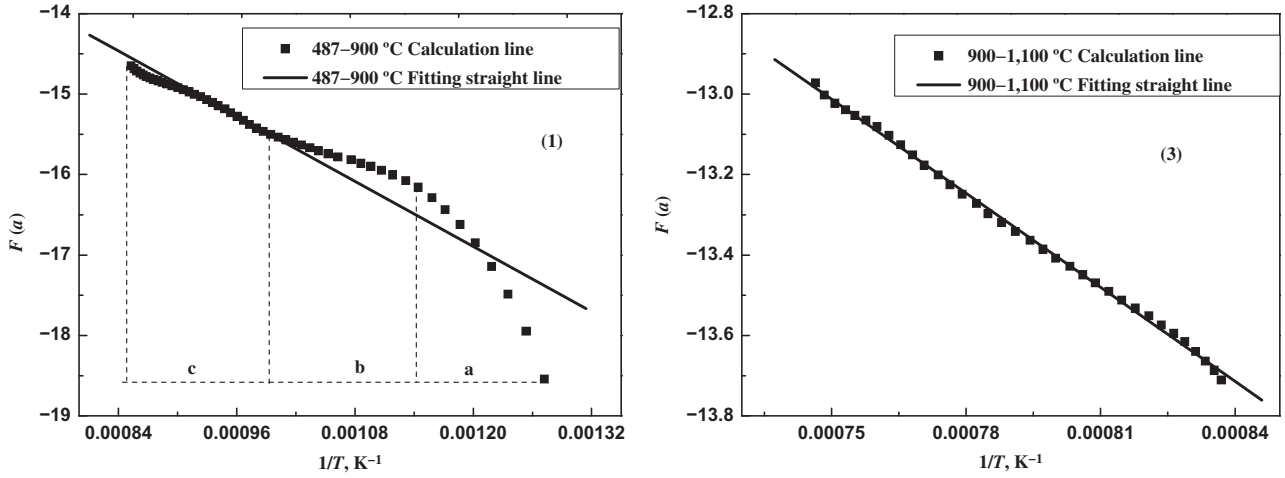

Figure 10: Calculation curve and fitting straight line at (1) and (3) stages in oxygen blast furnace.

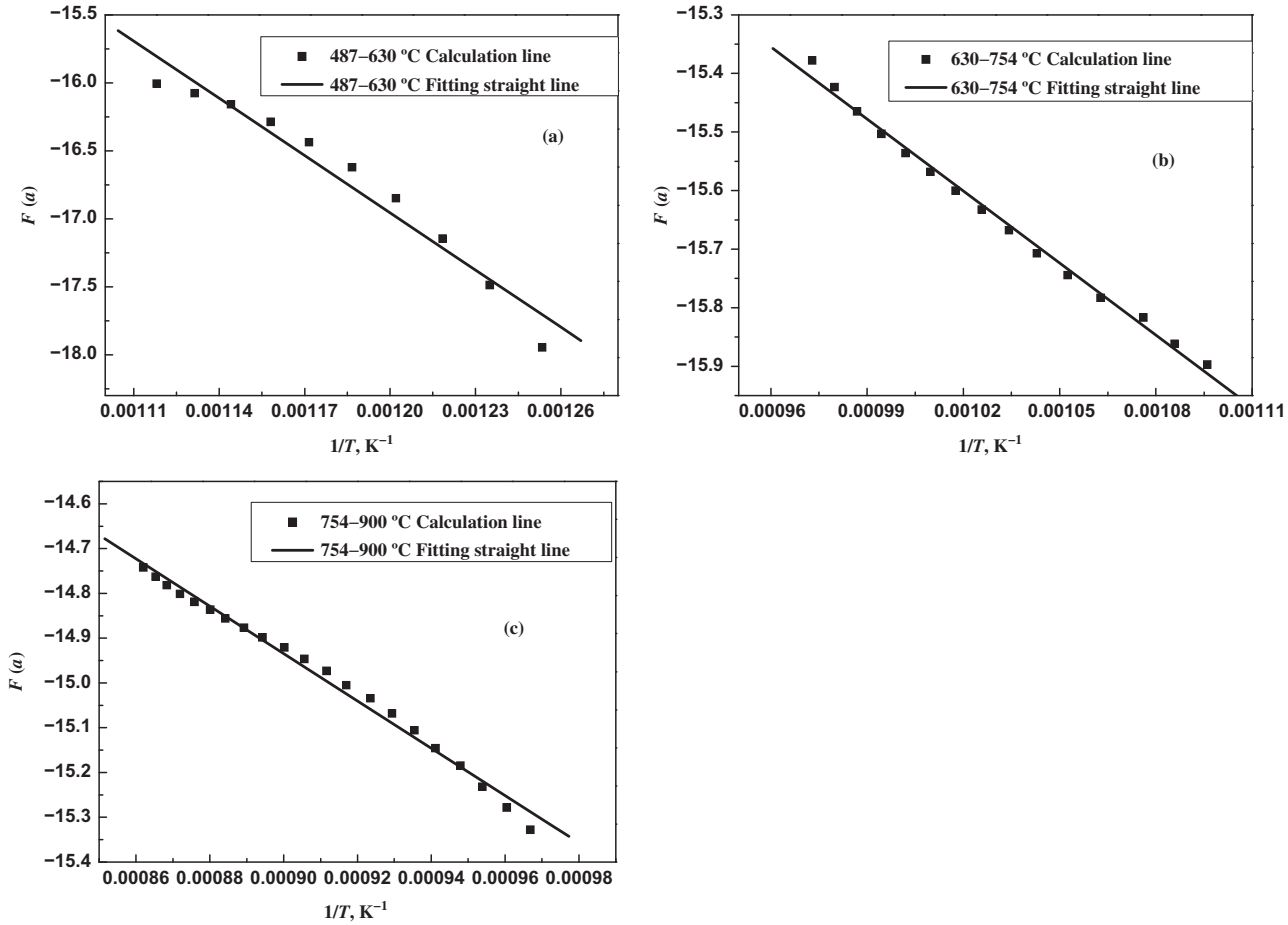

Figure 11: Three-stage calculation curves and fitting straight lines at 487–900 °C.

Table 4: Fitting results at different stages in oxygen blast furnace.

Temperature range	*a*	*b*	*E* (kJ mol^{-1})	*A*	*R*
487–630 °C	−0.11887	−14,030.75 ± 1,082.38	116.652 ± 8.999	1,12,124	−0.9771
630–750 °C	−11.41846	−4,100.29 ± 91.45	34.090 ± 0.760	0.406	−0.9968
750–900 °C	−10.1815	−5,281.07 ± 119.57	43.907 ± 0.994	1.799	−0.9952
900–1,100 °C	−7.1688	−7,791.50 ± 51.41	64.778 ± 0.427	30.007	−0.9993

The relevant parameters in calculation curves and fitting straight lines in OBF at different stages are shown in Table 4. It is found that the trends of the apparent activation energy in OBF are different to that in TBF. The activation energy at initial reaction in OBF reaches 116.652 kJ mol^{-1}, which is lower than 51.59 kJ mol^{-1} compared with that in TBF. It is due to the fact that the improvement of reduction potential in OBF reduced the reaction energy barrier. With the rise of temperature, the activation energy decreased to 34.090 kJ mol^{-1} at 630–754 °C.However, the activation energy is slightly higher to 43.907 kJ mol^{-1} at 750–900 °C and it is 64.778 kJ mol^{-1} at 900–1,100 °C.

According to the corresponding relationships between the values of apparent activation energy and the rate controlling steps in Table 3, the data in Table 4 were analyzed as follow. At the initial reaction stage, the apparent activation energy is 116.652 kJ mol^{-1} > 90 kJ mol^{-1}. It is similar to that in TBF and the controlling step is solid diffusion. When the reaction proceeds and the temperature increases, the apparent activation energy decreases to 34.090and 43.907 kJ mol^{-1}. This shows that, compared with that in TBF, the activated molecule increases and the reaction is easier. It is the mixed controlling step of gas diffusion and interfacial reaction. The reason for the different controlling step with that in TBF is that, with the increase of reduction potential, the reaction is promoted. The resistance of interfacial chemical reaction decreases and the resistance of gas diffusion increases. So the controlling step changes from interfacial reaction to mixed controlling. However, the apparent activation energy increases to 64.778 kJ mol^{-1} at 900–1,100 °C. The controlling step is interfacial reaction. This is estimated to be due to the fact that the H_2 and CO content in OBF are higher than that in TBF. The literature [20] has noted that the apparent rate constants were determined to be 33, 8.6 and 15 for the reduction of wustite with H_2, CO and H_2–CO mixture, respectively. The gas diffusion is easier in OBF. Meanwhile, the conversion rate reached to 0.795 after 900 °C insulation stage. It indicates that iron oxide has been reduced to wustite and has certain metallic iron. The residual iron oxides in the form of complex compounds as in Figure 1 are relatively difficult to reduce. So the overall controlling step at this stage is interfacial reaction.

At the 900 °C insulation stage for 30 min in OBF, the controlling step was determined according to the unreacted core model. Make the line $1-(1-a)^{\frac{1}{3}}$ versus t and $1-3(1-a)^{\frac{2}{3}}+2(1-a)$ versus t. The results are shown in Figure 12. Based on the fitting situation, the controlling step in insulation stage is interfacial reaction and gas diffusion.

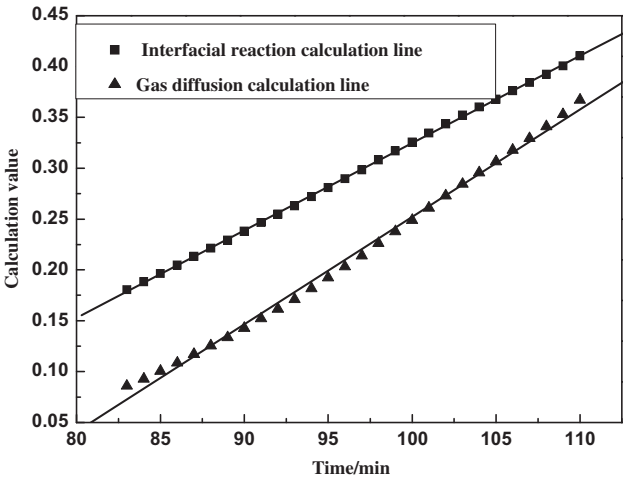

Figure 12: Fitting results of gas diffusion and interfacial reaction at the insulation stage in oxygen blast furnace.

Within the entire temperature range, the transition temperature points of the controlling step are 630 °C and after 900 °Cinsulation. Below 630 °C, the controlling step is solid diffusion; between 630 °C and the 900 °C insulation zone, it is the mixed control of interfacial reaction and gas diffusion; from 900 °C to 1,100 °C, it is interfacial reaction.

Conclusions

(1) In the condition of TBF, by using the method of Coats–Redfern, the non-isothermal reduction pellet was studied. The variation of apparent activation energy is 168.243 kJ mol^{-1}→50.554 kJ mol^{-1}→27.195 kJ mol^{-1}.

The corresponding controlling steps are solid diffusion→interfacial reaction→gas diffusion + interfacial reaction→gas diffusion. The transition temperatures of the controlling step are 750 °C and 900 °C.

(2) Compared with that in TBF, the variation of apparent activation energy in OBF is 116.652 kJ mol^{-1}→34.090 kJ mol^{-1}→43.907 kJ mol^{-1}→64.778 kJ mol^{-1}. Because of the increasing of reaction potential, the activation energy at the initial stage is lower than that in TBF. However, it is higher at the late stage due to the big rise of reduction degree. The corresponding controlling steps are solid diffusion→gas diffusion + interfacial reaction→interfacial reaction. The transition temperature of the controlling step in OBF is 630 °C (earlier 120 °C than in TBF) and after the 900 °C insulation. Based on the result of dynamics, pellet in lump zone can be reduced earlier in OBF and bring down the direct reduction degree, which is benefit for the carbon saving.

Funding: The authors gratefully acknowledge the financial support from Natural Science Foundation of China and Baosteel under grant no. 51134008 and National Basic Research Program of China (973 Program) (no. 2012CB720401).

References

[1] C.B. Xu and D.Q. Cang, J. Iron Steel Res. Int., 10 (2010) 1–7.
[2] Y.H. Han, J.S. Wang and Y.Z. Li, J. Univ. Sci. Technol. B, 33 (2011) 1280–1286.
[3] H. Yamaoka and Y. Kamei, ISIJ Int., 32 (1992) 709–715.
[4] M.A. Tseitlin, S.E. Lazutkin and G.M. Styopin, ISIJ Int., 34 (1994) 570–573.
[5] G. Zuo and A. Hirsch, Proceedings of the 4th ULCOS seminar, SP10-Top Gas Recycling Blast Furnace/n 2–3, October 1–2, Sweden (2008), pp. 1–6.
[6] G. Danloy, J. van der Stel and P. Schmole, Proceedings of the 4th ULCOS seminar, SP10-Top Gas Recycling Blast Furnace/n 2–1, October 1–2, Sweden (2008), pp. 1–3.
[7] Q.R. Ge, Kinetics of Gas-Solid Reaction. Atomic Energy Press, Beijing (1991).
[8] S. Vyazovkin and C.A. Wight, Int. Rev. Phys. Chem., 17 (1998) 407–433.
[9] R.Z. Hu, Thermal Analysis Kinetics (2nd ed.), Science Press, Beijing (2008).
[10] Z. Xiaojian, W. Jingsong and An. Xiuwei, J. Iron Steel Res. Int., 20 (2013) 12–18.
[11] W. Pan, K. Wu and X. Zhao, J. Univ. Sci. Technol. B, 35 (2013) 35–40.
[12] A. Kemppainen, O. Mattila and E.P. Heikkinen, ISIJ Int., 52 (2012) 1973–1978.
[13] K. Piotrowski, K. Mondal and T. Wiltowski, Chem. Eng. J., 131 (2007) 73–78.
[14] Y. Meiqin, Y. Jian and G. Feng, CIESC J., 64 (2013) 2072–2079.
[15] Z. Huang, K. Wu and B. Hu, J. Iron Steel Res. Int., 19 (2012) 1–4.
[16] M. Ettabirou, B. Dupre and C. Gleitzer, Steel Res. Int., 57 (1986) 306–312.
[17] M. Ettabirou, B. Dupre and C. Gleitzer, Metall. Mater. Trans. B, 19B (1988) 311–317.
[18] X.J. Wan, Acta Metall. Sin., 3 (1958) 197–209.
[19] J.H. Liu, Z. Jiayun and Z. Tuping, J. Iron Steel Res., 12 (2000) 5–9.
[20] H. Ono-Nakazato, T. Yonezawa and T. Usui, ISIJ Int., 43 (2003) 1502–1511.